Leadership in Sustainable Infrastructure
Leadership en Infrastructures Durables

Vancouver, Canada
May 31 – June 3, 2017/ *Mai 31 – Juin 3, 2017*

AN INTRODUCTION AND MODELING OF NOVEL SHAPE MEMORY ALLOY-BASED BRACING

Zareie, Shahin [1,5], M. Mirzai, Nadia [2], Alam, Shahria [3], and Seethaler, Rudolf J.[4]
[1] Graduate Research Assistant, EME 3204, School of Engineering, The University of British Columbia, Kelowna, BC, Canada
[2] Graduate Research Assistant, School of Civil Engineering, University of Tehran, Tehran, Iran
[3] Associate Professor, EME 4205, School of Engineering, The University of British Columbia, Kelowna, BC, Canada
[4] Associate Professor, EME 4205, School of Engineering, The University of British Columbia, Kelowna, BC, Canada
[5] kishoare.tamanna@alumni.ubc.ca

Abstract

The shape memory alloy has exceptional characteristics such as the superelasticity and shape memory effect, which enable it to undergo large deformation and then recover its predefined shape (initial state). Due to these specifications, the innovative shape memory alloy (SMA)-based bracing system is introduced to implement into the steel frame. The configuration of the smart bracing system supplies the damping force and dissipates the energy of seismic loads in compressive and tensile modes.
The numerical model of the smart bracing system is obtained by using the Open System for Earthquake Engineering Simulation (OpenSees). The model is validated by experimental results. Then, the numerical model is tested under the cyclic loads to examine the performance of the smart system**.**

1. Introduction

Shape Memory Alloys are non-conventional materials that have been implemented into civil infrastructures to improve seismic performance. Superelasticity and shape memory effect are unique characteristics of SMAs that enable them to recover the original state after being subjected to large strain up to 14% by removing stress or applying heat(Parulekar et al. 2012),(Hedayati Dezfuli & Alam 2013). Thus, researchers used SMAs to develop passive systems for structural control. Krumme (Krumme et al. 1995) explored the center-tapped (CT) device for civil structural applications; the unique features were reported such as increased damping, high energy dissipation capacity, corrosion resistance, low fatigue properties and temperature insensitivity. Parulekar et al.(Parulekar et al. 2012) introduced the NiTi damper and installed it in the six-story steel frame with dump tanks to control the seismic behavior. The study showed that the damper absorbed the energy of the earthquake load and increased the damping of structure.
Haque et al. (Haque et al. 2015) suggested a Piston Based Self-Centering (PBSC) bracing system based on SMA material. The system produced a resistance force in tensile and compression modes without buckling. The finite element model by Abaqus was performed to analyze the hysteresis response of PBSC under quasistatic loading. The hysteresis response proved that the re-centering ability appeared during the unloading phase and the system dissipated energy was remarkable.
The SMA-based devices were also tested in building numerically and/or experimentally to monitor the performance of the system independently and in comparison to the conventional systems. Massah et al. (Massah & Dorvar 2014) utilized SMA-based vertical links into eccentric bracing. The system was evaluated

after installation into 4, 9 and 14-story steel frames under cyclic loading. The result revealed the maximum relative displacement and residual deformation were reduced in all steel frames. Asgarian et al. (Asgarian & Moradi 2011) suggested four types of SMA bracing systems in steel frames. An evaluation of the seismic performance of the bracing systems was achieved by nonlinear time history analysis. The investigation showed that residual roof displacement and peak inter-story drift were smaller compared to buckling-restrained braced frames (BRBFs). Moradi et al.(Moradi et al. 2014) investigated the buckling-restrained SMA bracing system to mitigate the seismic hazards of the steel frame. They used OpenSees to model for buckling-restrained braced frames(BRBFs) and four different types of SMA bracing systems including V, inverted-V, X, and diagonal configurations of four-story steel frames and conduct the incremental dynamic analysis(IDA for all of them. The study showed that the damage level, including maximum Inter-storey drift (MID), remarkably reduced under different ground motions (GMs). In contrast to BRBF, the SMA-bracings supplied more maximum base shear force and higher stiffness.
In this study, the novel SMA bracing system is proposed for civil infrastructure to enhance structural behavior. In order to investigate the influence of the new bracing on structural response, the OpenSess is used to model a diagonal steel SMA bracing system and a BRBF in a four-story steel frames and compare together. The simplicity, functionality, and ease of manufacturing and installation are some of advantages of this system

1.1 Shape memory alloy

The shape memory alloys refer to a new group of material alloys with the capability of returning to their original shape by applying enough heat (Dolce, Mauro and Cardone, Donatello and Marnetto 2000). It is called shape memory effect (SME), which was discovered by Swedish physicist, Arne First, in 1932. Later, in 1958, the SME was found in nickel-titanium (NiTi) alloy accidentally in the U.S. Naval Ordnance Laboratory. In 1970, commercial application devices were available(Dolce, Mauro and Cardone, Donatello and Marnetto 2000) Currently, SMAs are available in different alloys such as Ag-Cd, Au-Cd, Cu-Al-Ni, Cu-Sn, NiTi, and so on(Dolce et al., 2000).
In addition, reversing the phase occurs by removing loads, which is called superelasticity. In this study, it is assumed that the superelasticity is the only parameter that causes SMA to recover it initial state. Figure 1 shows the hysteresis response of the superelasticity of SMAs schematically. In this response, two phases are available: 1. forward phase 2. reverse phase(Sharabash & Andrawes 2009). The forward phase (loading phase) begins after the elastic response of SMA that is an Austenite start strain (ε_{as}) If the strain becomes greater than ε_{as} , SMAs' behavior changes from elastic state to inelastic state and surges from ε_{as} to ε_{af} (Austenite finish strain). ε_{af} Is equal with $\varepsilon_{\max}$ which is the maximum reversible strain. Otherwise, the strain is a permanent strain. In this research, it is assumed that the applied strain is always less than ε_{mf} .

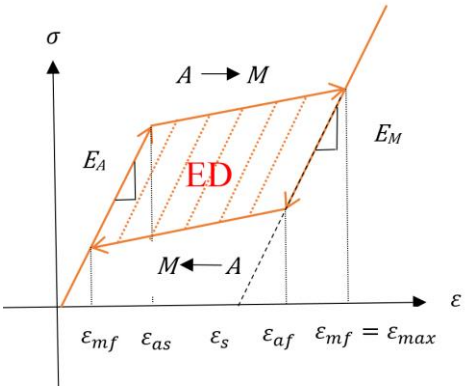

Figure 1. The hysteresis response of SMA

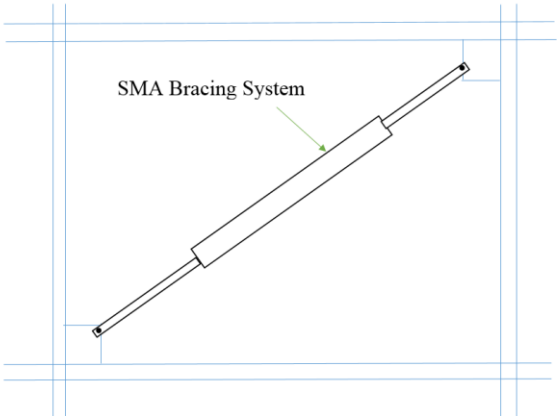

Figure 2. The installation sample of SMA bracing system

In the unloading phase, If the strain declines from ε_{af} , stress decreases proportionally to the applied strain until it passes the first point of the unloading phase, which is called the Austenite start strain (ε_{as}). If the strain becomes less than ε_{as} , it cuts down to reach to the Austenite finish strain (ε_{af}) and the stress reduces respectively; it is the last point of the Martensite to the Austenite phase. Any further reduction of the strain causes the stress to lessen and move back to the original state. In Figure 1, E_A is the elastic modulus in the Austenite phase and E_m is the elastic modulus in the Martensite Phase and ε_s is the maximum superelastic strain.

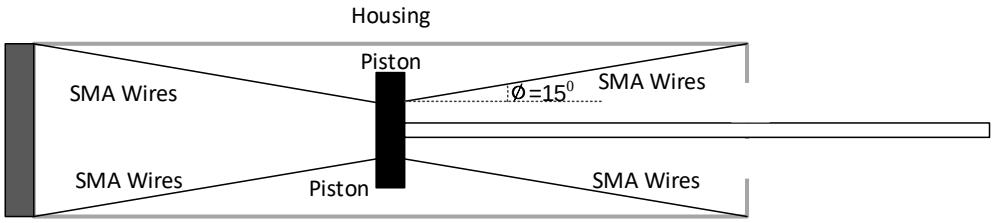

Figure 3. The conceptual design of SMA bracing

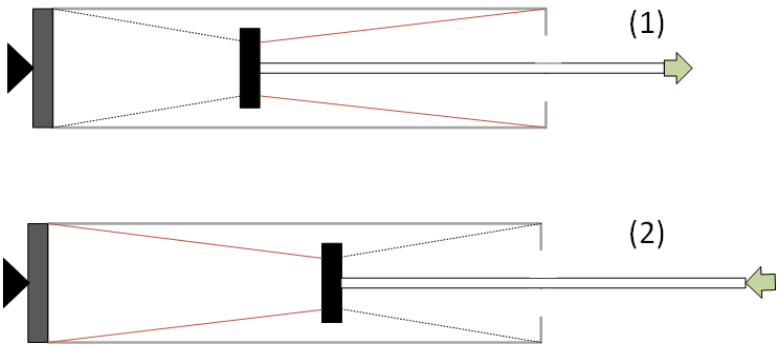

Figure 4. The operational mechanism of SMA bracing system

1.2 SMA bracing system

The proposed SMA bracing system is shown in Figure 2. The simplified model of the system is illustrated in Figure 3. The system is composed of a hollow cylinder, SMA wires, piston and plates. The operational mechanism is displayed in Figure 4. In the tension mode, the left side SMA wires provide damping force and in the compression mode the right side SMA wires produce resistance force. The seismic loads move civil infrastructure to both sides; this means that the installed system (as illustrated in **Error! Reference source not found.**) dissipates the energy of earthquake loads in both sides, which is an advantage of this system.
Table 1 displays the specifications of the SMA-based system, it consists of 100 SMA wires on each side and each SMA wire has a 1700 mm length for each side.

Table 1. The dimensions of the SMA bracing system

Bracing SMA material	Length(mm)	Radius of piston base(mm)	Thickness of Piston(mm)	Number of SMA wires	Angle(°)
NiTi	3410	50	10	100	15

1.3 Frame specification

The performance of the SMA-based system is evaluated in a steel frame, which was developed originally by Asgarian et al. (Saber Moradi , M. Shahria Alam 2014). The height of each story is 3.2 m and the length of the bay is 6 m.
Figure 5 schematically displays the steel frame with the embedded diagonally bracing system. The specifications and dimensions of this frame are illustrated in Table 2. The Roof Beam and the other stories' Beams are IPE30 and IPE36, respectively. C1 of the first and second floor is IPB200 and for the third and fourth floor is IPB140. C2 of the first and second floor is IPB220 and for the third and fourth floor is IPB160.

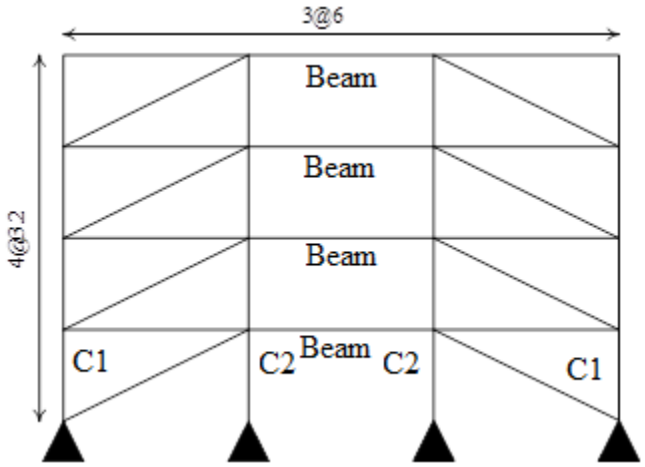

Figure 5. The Schematic diagram of steel frame with a diagonal bracing system (adapted from Saber Moradi , M. Shahria Alam, 2014))

Table 2. Model characteristics of four steel frame with bracing system (adapted from Saber Moradi , M. Shahria Alam, 2014))

Bracing type / Story	Diagonal SMA Bracing system					Diagonal BRBF				
	C1	C2	Beam	Area	Bracing material	C1	C2	Beam	Area	Bracing material
1	IPB200	IPB220	IPE360	3936.9	NiTi	IPB200	IPB220	IPE360	425	Steel
2	IPB200	IPB220	IPE360	3546.73	NiTi	IPB200	IPB220	IPE360	375	Steel
3	IPB140	IPB160	IPE360	3546.73	NiTi	IPB140	IPB160	IPE360	300	Steel
4	IPB140	IPB160	IPE300	3546.73	NiTi	IPB140	IPB160	IPE300	200	Steel

1.4 Material

The mechanical properties of the steel and SMA are shown in Table 3 and Table 4. The yield stress of the steel is about 235 MPa and the elastic modulus is 200 GPa.

$\varepsilon_{\max}$ of SMA is about 6 % and ε_s is 4.6 %. These are two parameters of SMA that show the superelasticity effect. In this paper, it is assumed that the temperature is greater than A_f to neglect the SME.

Table 3. The mechanical properties of steel

Alloy	Density (kg/m^3)	Elastic Modulus (GPa)	Poisson's Ratio	Yield Strength (MPa)	Reference
Steel	7850	200	0.3	235.36	(Moradi et al. 2014)

Table 4. The SMA properties

Alloy	$\varepsilon_{\max}(\%)$	$\varepsilon_s(\%)$	$E_A(Gpa)$	$A_f(^o c)$	Reference
NiTi	6	4.6	28	53	(Hedayati Dezfuli & Alam 2013)

1.5 Modeling

In order to model and analyze the bracing system and the steel frame, OpenSees(the Open System for Earthquake Engineering Simulation) software, which is specially designed for finite applications in civil infrastructures, is used(Asgarian & Moradi 2011).
Figure 6 displays the “steel02”, that is Giuffré-Menegotto-Pinto model with isotropic strain hardening and is chosen from the library of this software to model materials of beams and columns. Figure 7 llustrates “steel01” which is the uniaxial bilinear steel material with kinematic hardening used for braces.

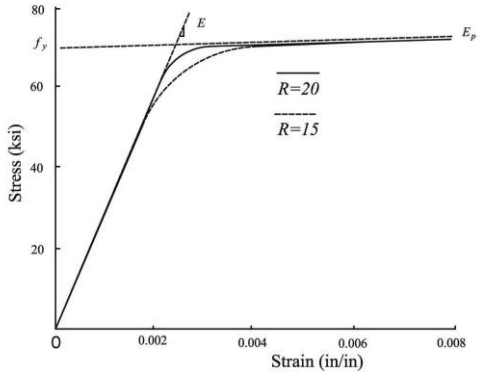

Figure 6. Steel 02 in OpenSess

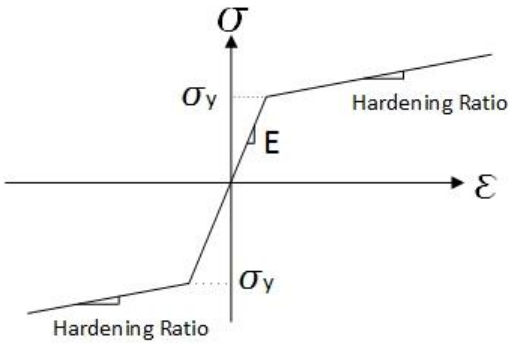

Figure 7. Steel 01 in OpenSess

The force-based nonlinearBeamColumn element with distributed plasticity and plastic hinge integration and fiber sections are used to model all mentioned elements. All beams and braces are simulated as a pined end element by considering the ZeroLength element with rigid material in translational directions. The floor behaves as a rigid diaphragm using the equalDOF command. Rayleigh damping with damping coefficient

5% is applied to the model. The dead and live loads considered for the model are 6 kN/m and 2 kN/m, respectively.

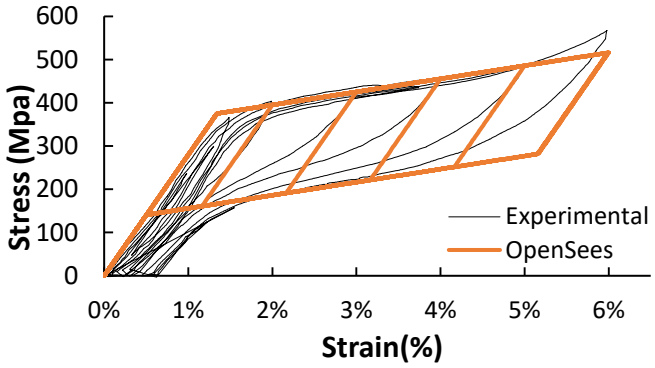

Figure 8. The comparison between hysteresis response of experimental and OpenSees

To model the SMA bracing system, the uniaxial self-centering (flag-shaped) material is chosen from the library material of OpenSess and tuned with respect to the NiTi experimental result(Dezfuli & Alam 2013). Figure 8 shows the comparison between the OpenSess and the experimental results.

1.6 Results

In order to evaluate the bracing systems, the AISC protocol load, as shown in Figure 9, is considered to excite the four story steel frames with embedded diagonal BRBF and SMA bracing system (Okazaki et al. 2005).

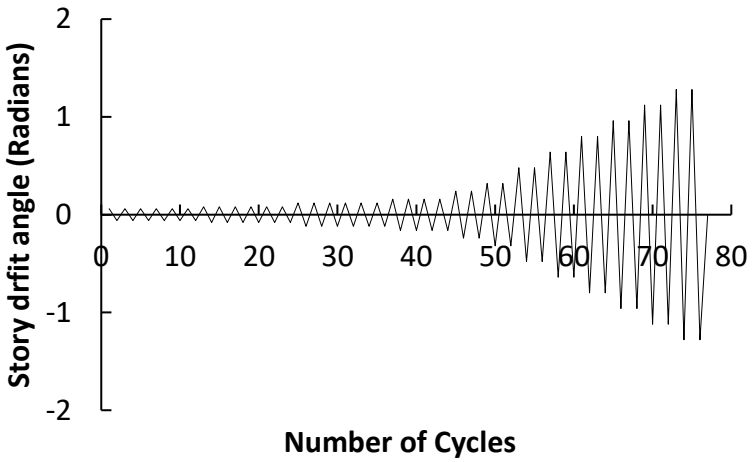

Figure 9. The AISC protocol loading

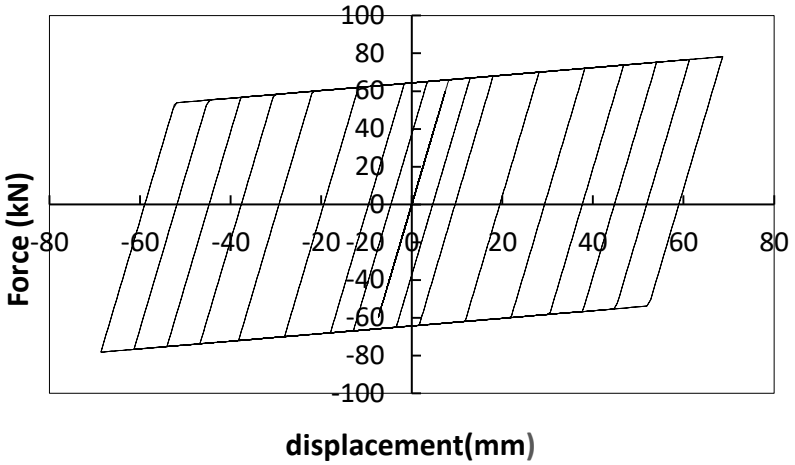

Figure 10. The hysteresis responses of the second history in steel frame equipped with BRBF bracing system

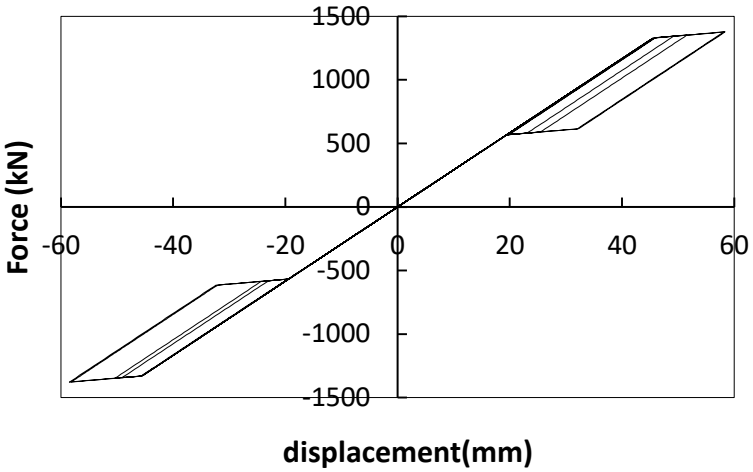

Figure 11. Hysteresis responses of the second history in steel frame equipped with SMA bracing system

The hysteresis responses of the second story of steel frames with both bracing systems are illustrated in

Figure 10 and Figure 11. It is observed that the amount of energy dissipation of the steel frame with the BRBF bracing system is clearly greater than the steel frame with the SMA bracing system. This occur because the steel bracing goes to inelastic response before the SMA bracing system with respect to its yield stress

It is also found that the re-entering ability of the SMA bracing system is much more than the BRBF system. This is due to the different behaviour of steel and SMA in the inelastic phase, which is the irreversible phase for steel and the reversible phase for SMA.

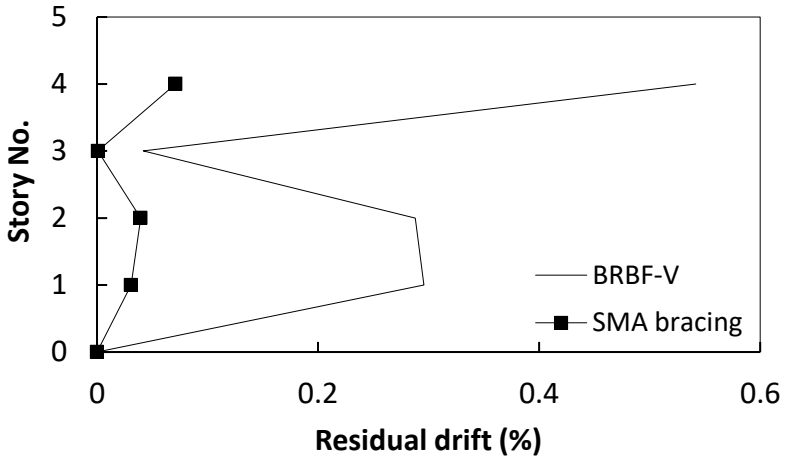

Figure 12. The residual drifts along stories with SMA and BRBF bracing system

The main feature of the SMA bracing system is shown in Figure 12. The superelasticity of the SMA-based system reduces the residual drift remarkably compared with the other one. The maximum residual drift is less than 0.1% which occurs in the fourth story of steel frame with SMA system, but it increases to 0.55% in the same story with the BRBF system. Overall, the residual drifts because of the SMA bracing system along the stories are less than the residual drifts that result from the BRBF system.

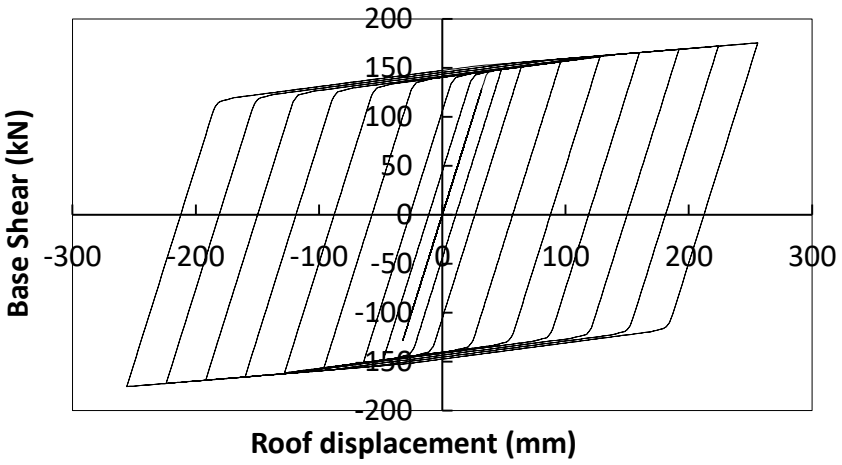

Figure 13. Roof displacement vs. Base shear of steel frame equipped with the BRBF bracing system

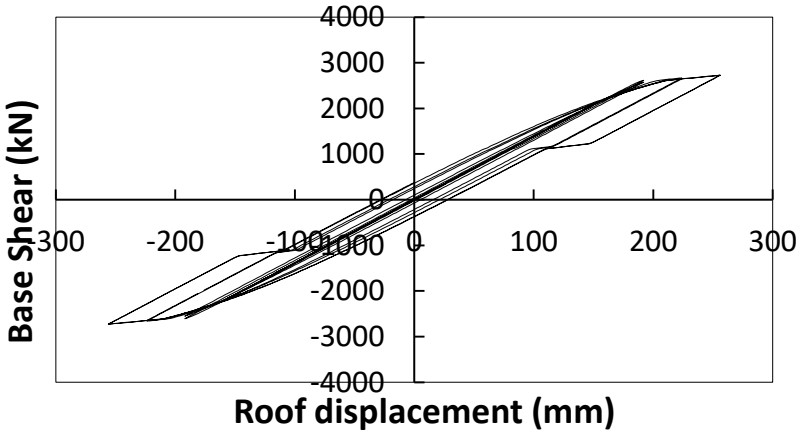

Figure 14.Roof displacement vs. Base shear of Steel frame equipped with the SMA bracing system

Figure 13 and Figure 14 show the base shear versus roof displacement. As can be seen, the BRBF has a significant residual roof displacement while the residual roof displacement in the SMA bracing system is much less than BRBF.

1.7 Conclusion

In this paper, the novel SMA bracing system is proposed to utilize in buildings. The main features are as follows:

1. The manufacturing of SMA system is more expensive than steel bracing; however the re-centering capability and the energy dissipation capacity of the SMA help to prevent the demolishing of the structure during the earthquake events. Thus, in compared to construction cost of structure, the system reveals the bold advantage.
2. The main advantage of the SMA-based system is the re-centering capability after remove of loading. The hysteresis response of the second floor, as a sample, and the residual drifts for each story are investigated
3. The roof displacement of steel frame with the SMA-based system is surprisingly lower than one with BRFB.
4. The energy dissipation capacity of steel increased due the material properties and design of the steel-based system.
   In future works, it is also recommend that pre-straining of SMA wires is applied to increase the amount of energy dissipation and optimize the design of the bracing system

Acknowledgements

The authors wish to thank the support provided by the University of British Columbia-Okanagan and the University of Tehran.

Reference

Asgarian, B. & Moradi, S., 2011. Seismic response of steel braced frames with shape memory alloy braces. *Journal of Constructional Steel Research*, 67(1), pp.65–74.

Dezfuli, F.H. & Alam, M.S., 2013. Shape memory alloy wire-based smart natural rubber bearing. *Smart Materials and Structures*, 22(4), pp.13–45.

Dolce, Mauro and Cardone, Donatello and Marnetto, R., 2000. Implementation and Testing of assive Control Devices Based on Shape Memory Alloys. *Earthquake Engineering \& Structural Dynamics*, 29(7), pp.945--968.

Haque, A.B.M.R., Alam, M.S. & The Structural Engineering Institute of the American Society of Civil, E., 2015. Cyclic performance of a piston based self-centering bracing system. *Structures Congress 2015*, pp.2360–2371. Available at: http://www.scopus.com/inward/record.url?eid=2-s2.0-84929246153&partnerID=40&md5=ec4e756fa15df20a6e4b1ba2c296926f.

Hedayati Dezfuli, F. & Alam, M.S., 2013. Shape memory alloy wire-based smart natural rubber bearing. *Smart Materials and Structures*, 22(4), p.45013. Available at: http://stacks.iop.org/0964-1726/22/i=4/a=045013.

Krumme, R., Hayes, J. & Sweeney, S., 1995. Structural damping with shape-memory alloys: one class of devices. In *Smart Structures & Materials' 95*. pp. 225–240.

Massah, S.R. & Dorvar, H., 2014. Design and analysis of eccentrically braced steel frames with vertical links using shape memory alloys. *Smart Materials And Structures*, 23(11).

Moradi, S., Alam, M.S. & Asgarian, B., 2014. Incremental dynamic analysis of steel frames equipped with NiTi shape memory alloy braces. *The Structural Design of Tall and Special Buildings*, 23(18), pp.1406–1425.

Okazaki, T. et al., 2005. Experimental study of local buckling, overstrength, and fracture of links in eccentrically braced frames. *Journal of Structural Engineering*, 131(10), pp.1526–1535.

Parulekar, Y.M. et al., 2012. Seismic response attenuation of structures using shape memory alloy

dampers. *Structural Control and Health Monitoring*, 19(1), pp.102–119.

Saber Moradi , M. Shahria Alam, B.A., 2014. Incremental dynamic analysis of steel frames equipped with NiTi shape memory alloy braces. *The Structural Design of Tall and Special Buildings*, 24(July 2014), pp.421–439.

Sharabash, A.M. & Andrawes, B.O., 2009. Application of shape memory alloy dampers in the seismic control of cable-stayed bridges. *Engineering Structures*, 31(2), pp.607–616. Available at: http://dx.doi.org/10.1016/j.engstruct.2008.11.007.